NeuroImage 184 (2019) 925–931

Contents lists available at ScienceDirect

NeuroImage

journal homepage: www.elsevier.com/locate/neuroimage

Glutamatergic facilitation of neural responses in MT enhances motion perception in humans

Michael-Paul Schallmo [a,*], Rachel Millin [a], Alex M. Kale [a], Tamar Kolodny [a], Richard A.E. Edden [b], Raphael A. Bernier [c], Scott O. Murray [a]

[a] Department of Psychology, University of Washington, Seattle, WA, USA
[b] Department of Radiology and Radiological Science, Johns Hopkins University, Baltimore, MD, USA
[c] Department of Psychiatry and Behavioral Sciences, University of Washington, Seattle, WA, USA

ARTICLE INFO

Keywords:
Functional MRI
Glutamate
Individual differences
MR spectroscopy
Vision

ABSTRACT

There is large individual variability in human neural responses and perceptual abilities. The factors that give rise to these individual differences, however, remain largely unknown. To examine these factors, we measured fMRI responses to moving gratings in the motion-selective region MT, and perceptual duration thresholds for motion direction discrimination. Further, we acquired MR spectroscopy data, which allowed us to quantify an index of neurotransmitter levels in the region of area MT. These three measurements were conducted in separate experimental sessions within the same group of male and female subjects. We show that stronger Glx (glutamate + glutamine) signals in the MT region are associated with both higher fMRI responses and superior psychophysical task performance. Our results suggest that greater baseline levels of glutamate within MT facilitate motion perception by increasing neural responses in this region.

1. Introduction

A direct relationship between greater neural responses and better perceptual functioning is well established in both humans (Boynton et al., 1999) and animal models (Britten et al., 1992; Newsome et al., 1989). One factor that may determine neural responsiveness and subsequent behavior is the amount of the neurotransmitter glutamate (Glu) available within a given region of cortex. Glu is the primary excitatory neurotransmitter in cortex and is released from presynaptic vesicles as the result of an action potential (Magistretti et al., 1999). Individuals with higher baseline Glu levels in a particular region may therefore possess greater potential for excitation within the local neural population (Conti and Weinberg, 1999). An index of Glu concentration can be measured non-invasively *in vivo* using MR spectroscopy (MRS). Although MEGA-PRESS sequences (Mescher et al., 1998) are most often used to measure γ-aminobutyric acid (GABA) levels, the difference spectrum that is obtained also contains a peak at 3.75 ppm associated with Glu. The size of this peak is believed to reflect the level of Glu within the MRS voxel, which is considered a stable individual trait. However, both Glutamine and Glutathione also contribute to the size of this peak (Harris et al., 2017; Mullins et al., 2014) – hence the peak is often referred to as Glx, to signify that it is a combined measure of multiple metabolites (glutamate, glutamine, & glutathione). Glutamine acts as a precursor to both Glu and GABA in the brain, and thus facilitates both neural excitation and inhibition (Albrecht et al., 2011), whereas glutathione plays an important role in protecting the brain against oxidative stress (Cooper and Kristal, 1997). Currently, it is not clear how Glx levels measured with MRS are related to the neural responses that support behavior.

We hypothesized that greater regional concentrations of Glx would be associated with higher neural activity (reflected in stronger fMRI responses) and in turn, superior performance on a task that depends on neural response magnitude. Our group recently examined the role of GABA during motion perception in humans using MRS (Schallmo et al., 2018). Here, we again chose to focus on neural processing within cortical area MT, in order to test our above hypothesis regarding a link between Glx, neural responses, and task performance. Neural responses within MT in both monkeys (Britten et al., 1992; Churan et al., 2008; Huk and Shadlen, 2005; Liu et al., 2016) and humans (Chen et al., 2017; Huk

Abbreviations: Glx, glutamate plus co-edited glutamine and glutathione, as measured by MR spectroscopy.

* Corresponding author. Present address: Department of Psychiatry, University of Minnesota, F212/2C West Building, 2450 Riverside Ave S, Minneapolis, MN, 55454, USA.
E-mail address: schal110@umn.edu (M.-P. Schallmo).

https://doi.org/10.1016/j.neuroimage.2018.10.001
Received 30 May 2018; Received in revised form 22 September 2018; Accepted 1 October 2018
Available online 9 October 2018

et al., 2001; Rees et al., 2000; Schallmo et al., 2018; Tadin et al., 2011; Turkozer et al., 2016) are known to be tightly linked to motion perception. In particular, studies in humans suggest that motion duration thresholds (Tadin, 2015; Tadin et al., 2003) – the amount of time that a stimulus needs to be presented to accurately discriminate motion direction – are shorter under conditions that elicit higher MT responses (Schallmo et al., 2018; Tadin et al., 2011; Turkozer et al., 2016), in agreement with our recent computational work (Schallmo et al., 2018). Motion perception is also thought to involve neural processing in other regions of early visual cortex (e.g., V1; Huk et al., 2001; Schallmo et al., 2018); thus, we sought to determine whether motion discrimination performance might be related to Glx and neural activity in area MT specifically, or in motion-responsive visual areas more generally.

Our current study consisted of three separate experimental sessions: 1) fMRI measurements of response amplitudes to visual motion, 2) psychophysical measurements of motion duration thresholds, and 3) MRS measurements of baseline Glx levels conducted while subjects watched a theatrical film. We obtained separate Glx measurements in two regions of visual cortex (which included areas MT and V1 respectively), as well as a control region in fronto-parietal cortex (the "hand knob"; Yousry et al., 1997). This allowed us to test whether relationships between Glx, fMRI, and psychophysics were specific to certain brain regions. Consistent with our hypothesis above, we observed a link between individual differences in Glx levels and fMRI response magnitudes within human MT complex (hMT+): individuals with higher Glx had higher fMRI responses. Further, we found that both higher Glx and larger fMRI responses in hMT+ were associated with reduced motion duration thresholds (superior performance). Overall, our findings suggest that individual differences in the amount of Glu, as measured by MRS, contribute to motion direction discrimination by facilitating neural responses within hMT+.

2. Materials and methods

2.1. Participants

Twenty-two young adults participated (mean age = 24 years, *SD* = 3.7; 13 females and 9 males). These subjects were included in two recent studies from our group examining the role of GABA in motion perception (Schallmo et al., 2018), and sex differences in motion processing (Murray et al., 2018). Subjects were screened for having normal or corrected-to-normal vision, no neurological impairments, and no recent psychotropic medication use. Further screening prior to MRS scanning included: no more than 1 cigarette per day in the past 3 months, no recreational drug use in the past month, no alcohol use within 3 days prior to scanning. Subjects provided written informed consent prior to participation and were compensated $20 per hour. All procedures were approved by the Institutional Review Board at the University of Washington (approval numbers 48946 & 00000556) and conformed to the guidelines for research on human subjects from the Declaration of Helsinki.

2.2. Visual display and stimuli

For fMRI, stimuli were presented using either an Epson Powerlite 7250 or an Eiki LCXL100A (following a hardware failure), both with 60 Hz refresh rate. Images were presented on a screen at the back of the scanner bore and viewed through a mirror mounted on the head coil. Images were shown using Presentation software (Neurobehavioral Systems, Berkeley, CA). For psychophysics, a ViewSonic PF790 CRT monitor (120 Hz) was used with an associated Bits# stimulus processor (Cambridge Research Systems, Kent, UK). Stimuli were presented on Windows PCs in MATLAB (MathWorks, Natick, MA) using Psychtoolbox-3 (Brainard, 1997; Kleiner et al., 2007; Pelli, 1997). Viewing distance for both displays was 66 cm, and display luminance was linearized.

The visual stimuli were identical to those described previously (Schallmo et al., 2018). Briefly, drifting sinusoidal luminance modulation gratings were presented with Gaussian blurred edges on a mean gray background. Grating contrast was either 3% or 98%. Gratings were 2° in diameter for fMRI, and 0.84, 1.7, & 10° in diameter for psychophysics. Spatial frequency was 1 cycle/° (fMRI) or 1.2 cycles/° (psychophysics). Drift rate was 4 cycles/s for both experiments.

2.3. Experimental procedure and data analysis

2.3.1. Functional MRI

The fMRI paradigm has been described previously (Schallmo et al., 2018). Structural (1 mm resolution) and functional data (3 mm resolution, 30 oblique-axial slices, 0.5 mm gap, 2 s TR) were acquired on a Philips 3T scanner. At the start of the fMRI scans, a 1-TR scan was acquired with the opposite phase-encode direction, which was used for distortion compensation.

The main fMRI scans measured the response to drifting gratings presented at different contrast levels within a blocked experimental design (Fig. 1A). Sixteen gratings were presented within each block

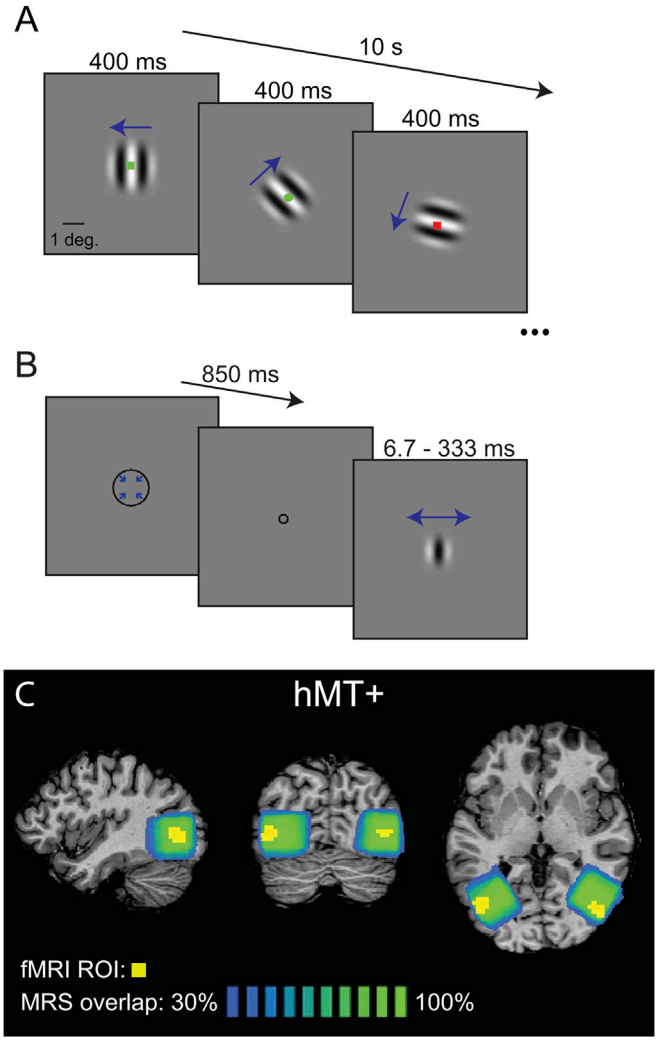

Fig. 1. Visual stimuli and MR spectroscopy. **A** shows the fMRI stimulus timing (10 s blocks of 400 ms drifting gratings). Blue arrows indicate motion direction. Fixation task stimuli also shown. **B** shows the timing of a psychophysics trial from the task performed outside the scanner (850 ms cue, variable grating duration). Average MRS voxel placement is shown in **C** (adapted from Schallmo et al., 2018). Green-blue color indicates the percent overlap of the fMRI-localized MRS voxels in the hMT+ region (in Talairach space) across all subjects. Average hMT+ ROIs from fMRI for all subjects are shown in yellow (threshold correlation between predicted & observed fMRI timeseries $r \geq 0.3$).

(400 ms duration, 225 ms inter-stimulus interval, 10 s total block duration), which drifted in 8 possible directions (randomized & counterbalanced). Stimulus contrast varied across block; this began with a 0% contrast (blank) block. Then, blocks of high (98%) and low contrast (3%) gratings were presented in alternating order, each followed by a blank block to allow the fMRI response to return to baseline (6 high, 6 low, and 13 blank blocks total). Task scans were 4.2 min long (125 TRs), and each subject completed a total of 2–4 scans across 1 or 2 scanning sessions (some subjects chose to end a scanning session early, or chose not to return for a second scanning session). This experiment was carried out as part of a larger set of visual fMRI experiments focused on the neural mechanisms of spatial suppression during motion processing, as recently described (Schallmo et al., 2018).

Functional localizer scans were also included in each scanning session, in order to identify regions-of-interest (ROIs). The first localizer was designed to identify human MT complex (hMT+); we did not attempt to distinguish areas MT and MST (Huk et al., 2002). Drifting gratings (as above, but 15% contrast) alternated with static gratings across blocks (10 s block duration, 125 TRs total). Bilateral hMT+ ROIs (averaged across subjects, in Talairach space) are shown in Fig. 1C (yellow). A description of the second localizer (used to define ROIs in early visual cortex) is provided in the Supplemental Information.

Subjects performed a fixation task during all fMRI scans. This involved responding to a green circle within a series of colored shapes presented briefly at fixation (Fig. 1A). This task encouraged subjects to focus their spatial attention at the center of the screen and minimized eye movements away from this position.

FMRI data were analyzed using BrainVoyager (Brain Innovation, Maastricht, The Netherlands), and MATLAB (The Mathworks, Natick, MA). Preprocessing was performed in the following order: motion correction, distortion compensation, high-pass filtering (2 cycles/scan), co-registration, and transformation into the space of the individual subject's T_1 anatomical scan. Normalization and spatial smoothing were not performed; all analyses were conducted within ROIs for each individual subject. ROIs were defined using correlational analyses (initial cluster thresholds of $r \geq 0.3$), taking the top 20 highest-correlating voxels as previously described (Schallmo et al., 2018). ROI position was verified on an inflated model of the white matter surface. Analyses of fMRI time course data were performed in MATLAB using BVQXTools. Data were broken into epochs spanning 4 s before the onset of each block to 2 s after the offset. Average baseline responses were calculated across blocks separately for each condition (3% & 98% contrast); this was computed as the average response to the blank background 0–4 s prior to block onset. Data were converted to percent signal change, averaged across blocks, across ROIs from each hemisphere, and then averaged across scanning sessions. Responses for each condition were defined as the mean of the fMRI signal peak (from 8 to 12 s following block onset). For the correlational analyses (i.e., Fig. 2C), fMRI responses to low and high contrast stimuli were averaged, as an index of overall responsiveness.

2.3.2. Behavioral psychophysics

Subjects performed a psychophysical motion direction discrimination task outside of the scanner, during a separate experimental session. This paradigm followed established methods (Foss-Feig et al., 2013; Tadin et al., 2003) and is described in a recent paper from our group (Schallmo et al., 2018). In the full experiment, drifting gratings were presented at 2 contrast levels (3% & 98%) and 3 sizes (0.84, 1.7, & 10° diameter).

In this task, subjects were asked to report whether a briefly presented grating drifted left or right (Fig. 1B). The stimulus duration was adjusted across trials (range 6.7–333 ms) using the Psi adaptive staircase method within the Palamedes toolbox (Kingdom and Prins, 2010; Prins and Kingdom, 2009), in order to find the duration for which motion discrimination performance reached 80% accuracy. Trials began with a brief central fixation mark (a shrinking circle; 850 ms), followed by the presentation of the grating. A fixation mark presented after the grating cued the subjects to respond; response time was not limited. Staircases were comprised of 30 trials for each stimulus condition (3% & 98% contrast), presented in a randomized counterbalanced order within each run. Run duration was approximately 6 min. Subjects completed 4 runs each, for a total experiment duration of about 30 min, including instructions and practice prior to the start of the main experiment.

Data from each staircase were fit with separate Weibull functions using the Palamedes toolbox (Prins and Kingdom, 2009). Motion duration thresholds were defined at 80% accuracy based on this fit. When averaging across thresholds from different conditions (i.e., for the correlations in Fig. 2D), the mean threshold was first taken across runs in each condition, and then the geometric mean was taken across conditions, to account for the fact that threshold ranges varied across conditions.

Measuring psychophysical motion duration thresholds for different contrast levels allowed us to probe the effect of stimulus contrast on motion discrimination, as shown in Fig. 2E. In order to minimize the effects of spatial suppression/summation seen with larger stimuli (Foss-Feig et al., 2013; Schallmo et al., 2018; Tadin, 2015; Tadin et al., 2003), only data from the smallest stimulus size were included in the analyses within the main text. Additional analyses of the medium and big sizes are included in the Supplemental Information. This decision was motivated by our observation that duration thresholds for medium and big drifting gratings did not consistently decrease with increasing contrast (Schallmo et al., 2018), unlike for the smallest size (Fig. 2E). Thus, we focused primarily on the smallest size condition, wherein motion discrimination performance is expected to depend primarily on the magnitude of responses driven by stimuli within the classical receptive field of neurons in motion-selective visual areas such as MT (Tadin, 2015).

2.3.3. MR spectroscopy

Our MRS data acquisition was the same as described previously (Schallmo et al., 2018). Briefly, we used a MEGA-PRESS (Mescher et al., 1998) sequence on a Philips 3T scanner. Sequence parameters were as follows: 3 cm isotropic voxel, 320 averages, 2048 data points, 2 kHz spectral width, 1.4 kHz bandwidth refocusing pulse, VAPOR water suppression, 2 s TR, 68 ms TE, 14 ms editing pulses at 1.9 ppm for "on" and 7.5 ppm for "off" acquisitions, "on" and "off" interleaved every 2 TRs with a 16-step phase cycle. Across 2 additional scanning sessions (separate from fMRI), MRS data were acquired from the following 3 regions: 1) lateral occipital cortex, centered on hMT+ (Fig. 1C); 2) mid-occipital region of early visual cortex (EVC), parallel to the cerebellar tentorium (Supplemental Fig. 1A); 3) fronto-parietal cortex (FPC), centered on the "hand-knob" (Yousry et al., 1997; Supplemental Fig. 1B). Voxels in hMT+ were positioned using an on-line functional localizer (moving vs. static, as above; identified using Philips iViewBOLD software, statistical threshold $t \geq 0.3$). For EVC and FPC, voxels were positioned based on each individual's anatomical landmarks. MRS data were acquired in left and right hMT+ for each subject, typically within the same scanning session. Data were acquired in EVC across 2 separate scans (typically in different sessions; 1 subject had only 1 EVC scan). Only 1 scan was acquired in FPC (1 subject did not complete the FPC scan). MRS, fMRI, and psychophysical data were collected within a 2-week period for all subjects. Because subject compliance is critical for high-quality edited MRS, participants watched theatrical films during spectroscopy data acquisition in order to reduce boredom and fatigue. Images were presented on the screen (as above, for fMRI), and audio was presented through MR-compatible headphones. Previous work suggests metabolite measurements from MRS reflect individual differences that are stable over the course of several days to months (Evans et al., 2010; Greenhouse et al., 2016; Near et al., 2014). Thus, we assume that metabolite values measured with MRS were unaffected by the presentation of audio and visual stimuli during the scan.

MRS data were analyzed using the Gannet toolbox version 2.0 (Edden et al., 2014). Automated processing steps within this toolbox were as follows: frequency and phase correction, artifact rejection (frequency

correction > 3 SD above the mean), and exponential line broadening (3 Hz). The Glx peak at 3.75 ppm was fit with a double-Gaussian function (Fig. 2A and B); the integral of this function served as the measure of Glx concentration. Note that this fitting was performed separately from fitting the GABA peak at 3 ppm. The value of Glx was scaled by the integral of the water peak for each individual. Correction for gray/white matter content within the voxel was not performed, as there is currently no standard within the field regarding such a correction of Glx levels (for relevant discussion of gray/white matter content correction of GABA, see Harris et al., 2015; Mullins et al., 2014). Instead, we performed the following statistical analyses to probe the possible confounds of water and gray/white matter content in our results.

No significant correlations were observed between the concentration of unsuppressed water (fit by Gannet) in hMT+ and either fMRI response magnitudes ($r_{20} = -0.37$, 2-tailed $p = 0.081$, FDR corrected for 2 comparisons of water) or psychophysical thresholds ($r_{20} = 0.44$, 2-tailed $p = 0.080$, FDR corrected for 2 comparisons of water). However, as these correlations were moderately strong (despite not reaching statistical significance), the effect of scaling Glx values to water merits further consideration. Since we observed qualitatively similar results to those presented below when scaling Glx to creatine instead of water (not shown), we believe it is reasonable to conclude that the observed correlations are driven by a genuine relationship between Glx, fMRI, and motion thresholds, rather than being attributable to water scaling. Further, using a linear regression approach we found that after factoring out the relationship with water, the residuals of the Glx signals in hMT+ showed qualitatively the same relationship with fMRI responses ($r_{20} = 0.47$, $p = 0.028$, FDR corrected for 2 comparisons of Glx with water factored out) and motion duration thresholds ($r_{20} = -0.37$, $p = 0.038$, FDR corrected for 2 comparisons of Glx with water factored out) as observed for the original Glx measurements. Finally, we found no significant correlations between fMRI or duration thresholds and the ratio of GM/WM within hMT+ ($r_{20} \leq 0.17$, uncorrected p-values ≥ 0.46), nor between Glx and the ratio of GM/WM in hMT+ ($r_{20} = 0.26$, uncorrected $p = 0.24$).

2.4. Statistics

Statistical analyses were performed in MATLAB. Glx values were averaged between left & right hMT+, and across the 2 EVC scans. Because variance differed for duration thresholds at low and high contrast, Friedman's non-parametric ANOVA was used to compare them, and the geometric mean was taken when averaging low and high contrast thresholds. When correlating different measures, fMRI responses and duration thresholds were each averaged across low and high stimulus contrasts to minimize multiple comparisons. In cases where multiple comparisons were made, false discovery rate (FDR) correction was used to adjust p-values. One tailed Pearson's correlation coefficients were calculated for all correlational analyses; this is justified by the strong *a priori* hypotheses being tested and is noted for each occurrence in the Results. Correlation significance was further examined using (non-parametric) permutation tests, which involved randomly shuffling the data being correlated across subjects in each of 10,000 iterations. The proportion of permuted correlations with coefficients greater (or more negative) than that of the observed, un-shuffled correlation served as the measure of significance (the p-value).

3. Results

Using MR spectroscopy, we measured the concentration of glutamate (plus co-edited metabolites; Glx; Fig. 2A and B) within a region of visual cortex that included the motion-selective area known as human MT complex (hMT+). We sought to determine whether individual differences in baseline Glx concentration in hMT+ were positively associated with neural responsiveness to visual motion, as indexed with fMRI. In a separate scanning session, fMRI signals were measured in hMT+ in response to moving gratings with low (3%) and high (98%) luminance contrast (Fig. 2C). Responses were larger for high than for low contrast stimuli (1-tailed paired $t_{21} = 8.02$, $p = 4 \times 10^{-8}$), as expected (Tootell et al., 1995). An overall index of fMRI responsiveness was obtained for each subject by averaging the peak response to both low and high contrast (gray regions; Fig. 2C). As predicted, there was a significant positive correlation between average fMRI responses in hMT+ and concentrations of Glx in the same region (Fig. 2D; $r_{20} = 0.54$, 1-tailed $p = 0.022$; FDR corrected for a total of 4 comparisons testing for correlations between Glx & fMRI or Glx & motion thresholds, see below). In contrast, no significant correlation was observed between fMRI responses and Glx measured in EVC (see Supplemental Fig. 1C). These results suggest that individuals with more Glx in the region that includes area MT have larger neural responses to moving stimuli, consistent with stronger glutamatergic excitation.

We next examined whether individual differences in Glx concentration in the hMT+ region were associated with behavioral differences in motion discrimination. In a psychophysical session outside the scanner, we measured motion duration thresholds (Tadin, 2015; Tadin et al., 2003) for drifting gratings (0.84, 1.7, and 10°) with low and high contrast (Fig. 2E). Duration thresholds were smaller for high vs. low contrast stimuli (Friedman's $X^2{}_1 = 30$, $p = 4 \times 10^{-8}$), consistent with previous findings (Foss-Feig et al., 2013; Tadin et al., 2003). To obtain an overall measure of motion perception, duration thresholds were averaged across low and high contrast. We observed the predicted relationship between Glx in hMT+ and average motion duration thresholds for small (0.84°) gratings; individuals with greater Glx showed lower thresholds (superior performance; Fig. 2F; $r_{20} = -0.44$, 1-tailed $p = 0.042$, FDR corrected for a total of 4 comparisons testing for correlations between Glx & fMRI or Glx & motion thresholds). A similar negative correlation with Glx in hMT+ was found when examining duration thresholds for medium sized (1.7°), but not for big (10°) gratings (Supplemental Fig. 2A & C). The relationship between duration thresholds and Glx was specific to hMT+; we saw no significant correlations between thresholds and Glx in two other MRS voxels (early visual cortex [EVC] and fronto-parietal cortex; $|r_{19\text{-}20}| < 0.23$, 1-tailed p-values > 0.27, FDR corrected for a total of 4 comparisons testing for correlations between Glx & fMRI or Glx & motion thresholds; Supplemental Fig. 1D and E).

The significant positive correlation between Glx and fMRI response magnitudes in hMT+, and the negative correlation between Glx and duration thresholds together suggest a negative relationship may exist between fMRI responses and duration thresholds. Indeed, we observed a significant negative correlation ($r_{20} = -0.60$, 1-tailed $p = 5 \times 10^{-4}$); higher averaged fMRI responses in hMT+ were associated with lower averaged duration thresholds for small gratings, as previously reported (Murray et al., 2018). Similar results were again observed for medium but not for big gratings (Supplemental Fig. 2B & D). Multiple linear regression analysis showed that duration thresholds for small gratings could be described by a combination of Glx & fMRI measures in hMT+, such that:

$$T = -33.9*Glx - 39.8*fMRI + 135.9 \quad (1)$$

where *fMRI* is the average response in hMT+ at low & high contrast, and T is the average duration threshold (geometric mean across contrasts). The linear relationship between Glx, fMRI responses, and thresholds was significant ($F_{2,19} = 5.89$, $p = 0.010$), with an R^2 value of 0.383. Taken together, our findings are consistent with the idea that stronger glutamatergic excitation drives larger neural responses in hMT+ during motion perception, thereby facilitating lower duration thresholds (i.e., superior motion discrimination).

The concentration of Glx showed some specificity between regions. Glx concentrations in hMT+ correlated to some extent with Glx in EVC, but this did not survive correction for multiple comparisons ($r_{20} = 0.43$, 1-tailed $p = 0.023$, uncorrected; $p = 0.069$ after FDR correction for 3

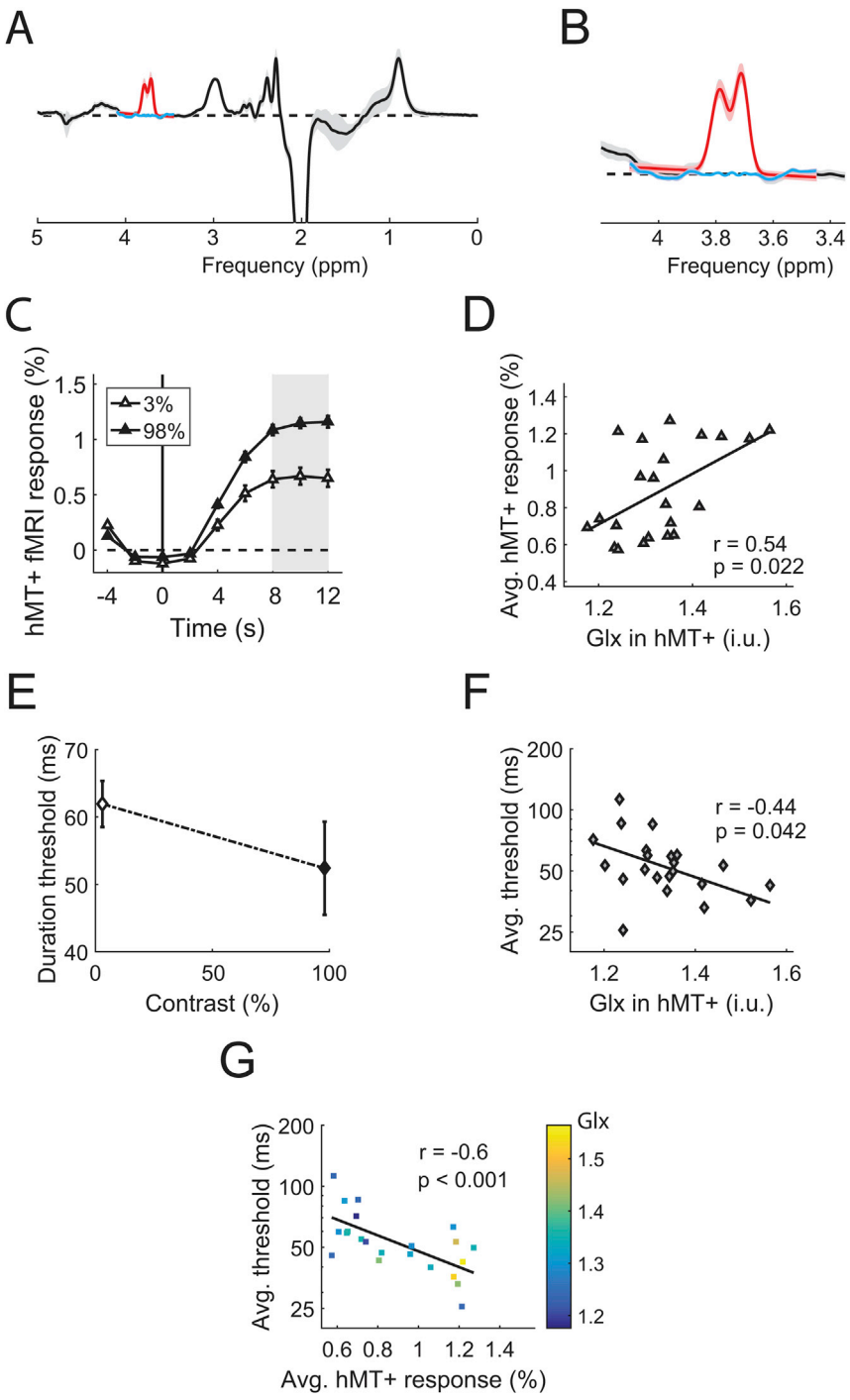

Fig. 2. A link between Glx, fMRI, and motion duration thresholds. **A** shows the MR spectra (black), fit Glx peak (red) and residuals (blue) averaged across subjects. Error bars in **A** & **B** are *SD*. **B** shows a zoomed view of the data from **A.** Panel **C** shows the time course of fMRI responses in hMT+, averaged across subjects. Peak response was calculated within the gray region. Higher Glx in hMT+ correlates significantly with greater fMRI responses in the same area (**D**; averaged across contrasts). Glx values are in institutional units (i.u.). Duration thresholds (**E**) correlated negatively with Glx in hMT+ (**F**; geometric mean of thresholds across contrasts). Error bars in **C** & **E** are *SEM*. **G** shows the correlation between fMRI in hMT+ and thresholds, with Glx levels indicated by color.

comparisons of Glx between regions). Neither hMT+ nor EVC concentrations were significantly associated with Glx in fronto-parietal cortex ($|r_{20}| < 0.37$, 1-tailed p-values > 0.097, FDR corrected for 3 comparisons of Glx between regions).

Recent work from our group has demonstrated a small but statistically reliable sex difference in motion discrimination thresholds, with females showing slightly higher duration thresholds on average than males (Murray et al., 2018). Thus, we examined whether there might be sex differences in Glx levels in hMT+ as well. However, no significant difference in hMT+ Glx was observed between males (mean = 1.33 i.u., $SD = 0.10$) and females (mean = 1.34 i.u., $SD = 0.10$; 2-tailed independent samples $t_{20} = 0.17$, $p = 0.87$). This is concordant with our recent finding (Murray et al., 2018) that fMRI response magnitudes in hMT+ also did not differ between sexes (despite the significant difference in psychophysical thresholds for the same subjects). The lack of a sex difference in Glx may reflect the fact that, although neural processing in MT clearly influences motion perception, response magnitudes in MT are not the only factor that determine duration thresholds for motion discrimination.

We also examined whether the observed relationships between Glx and fMRI or motion discrimination thresholds might in fact be attributable to GABA levels, possibly as an artifact of the MRS sequence. Although a Glx peak is obtained using MEGA-PRESS, this sequence is typically used to measure the concentration of an edited GABA peak at 3 ppm, which is acquired in the same scan (Mescher et al., 1998; Mullins et al., 2014). We have previously observed that higher GABA

concentrations in hMT+ correlate with lower motion discrimination thresholds within the same group of subjects (Schallmo et al., 2018). Thus, we sought to determine whether the current relationships with Glx might be accounted for by the previously reported relationship with GABA – perhaps due to homeostatic processes balancing the levels of these neurotransmitters, the manner in which they were measured together using MEGA-PRESS, and/or the method of quantifying both peaks in Gannet (Edden et al., 2014). However, we observed no significant correlations between Glx and GABA measurements across individuals in any of the 3 ROIs that we examined (not shown; all $|r_{(20)}| < 0.34$, 2-tailed p-values > 0.14; uncorrected), suggesting that the Glx results presented here cannot be explained by the amount of co-measured GABA.

Finally, we sought to determine whether our results might be attributed to individual differences in the size of hMT+. Since the hMT+ ROI occupied a small and variable proportion of the volume of the MRS voxel (Fig. 1C), we examined whether fMRI responses in hMT+ or motion duration thresholds might be associated with ROI size (rather than with Glx *per se*). We found that individuals with larger hMT+ responses also had larger ROIs ($r_{20} = 0.53$, 1-tailed $p = 0.010$, FDR corrected for 2 comparisons of ROI size), but there was no significant relationship between ROI size and motion duration thresholds ($r_{20} = 0.02$, 1-tailed $p = 0.54$, FDR corrected for 2 comparisons of ROI size). This suggests that individual variability in the size of hMT+ may not fully account for the observed 3-way association between Glx, fMRI responses, and motion perception.

4. Discussion

To our knowledge, this is the first study to present evidence of a 3-way link between behavioral performance, BOLD response magnitudes, and Glx levels in humans. These findings help to clarify the role of glutamate in visual motion perception, and suggest that higher excitatory tone (as measured by Glx from MRS) facilitates larger neural responses and greater perceptual sensitivity. These results are consistent with our recent computational work, which accounts for motion duration thresholds using a divisive normalization model (Schallmo et al., 2018). In this model framework, any increase in the strength of excitation (i.e., as a result of higher Glx levels) will necessarily yield larger predicted neural responses. This in turn will produce lower predicted values for motion duration thresholds, as we assume an inverse relationship between thresholds and response magnitudes within the model.

A straightforward association between higher levels of Glx, larger fMRI responses, and superior performance is perhaps not surprising. However, our findings are notable, given that the relationships between each of these measures and the underlying neural responses are complex (Duncan et al., 2014; Harris et al., 2015; Logothetis, 2008; Logothetis et al., 2001). Adding to this complexity, Glu also plays an important role in cell metabolism (Magistretti et al., 1999) in addition to functioning as a neurotransmitter. BOLD signals have been found to be more strongly associated with the strength of local field potentials (LFPs) vs. spike rates (Logothetis et al., 2001), and thus, fMRI responses may be more closely related to activity level within a local neural network than with the degree of spiking among pyramidal 'output' cells. Given such a relationship between fMRI and the underlying neural activity, our results suggest that higher levels of Glx may be linked to stronger excitation and greater local network activation.

It is still unclear how measures of Glx from MRS are tied to changes in neural activity in the human brain (Duncan et al., 2014). Studies using functional MRS at 7 T to measure Glu show increased occipital Glu following visual stimulation, and support the idea that the magnitude of Glu being measured depends on the level of local neural activity (Apšvalka et al., 2015; Lin et al., 2012; Mangia et al., 2007; Schaller et al., 2013). However, it is not yet known to what extent the Glu being measured with MRS reflects a 'direct' relationship with neural activity (i.e., driven by Glu neurotransmission) vs. an 'indirect' one (i.e., reflects Glu's role in cell metabolism, which is affected by spike rate). It has been argued that Glu becomes more MR visible as it moves from pre-synaptic vesicles to the synaptic cleft during neurotransmission and into astrocytes following reuptake, and that this change in MR visibility may suggest that Glx measured with MRS reflects Glu release during neurotransmission (Apšvalka et al., 2015). Alternatively, higher rates of neural activity might also increase the rate of Glu cycling through the synaptic cleft, which could lead to a transient buildup of Glu (depending on the rate limiting step in this cycle; Lin et al., 2012). While the 3-way association between Glx, fMRI, and behavior in the current study is consistent with the idea that Glx levels reflect the strength of glutamatergic neurotransmission, direct experimental support for this hypothesis remains lacking. Thus, we cannot rule out the possibility that the relationship we observed in hMT+ between Glx, fMRI, and motion thresholds may not be causal, but may instead be driven by one or more additional unknown factors.

Our work helps to clarify how glutamate in human visual cortex supports visual behavior. We are aware of very few studies examining how visual perception is related to individual differences in Glx measurements. Some have found that higher occipital Glx measurements are associated with increased visual functioning (Terhune et al., 2015; Wijtenburg et al., 2017), while others have not (Pugh et al., 2014; Takeuchi et al., 2017). One study from the latter category found that frontal Glx levels, but not measurements in MT, were associated with individual differences in an ambiguous motion perception task (Takeuchi et al., 2017). The discrepancy with the current findings may be explained by the manner in which visual behavior was assessed (i.e., ambiguous motion vs. direction discrimination). The association between lower motion duration thresholds (better performance) and greater Glx in MT from the current study suggests that motion discrimination performance is facilitated by higher levels of Glu, likely due to greater excitatory neural activity within area MT.

The role of area MT in visual motion perception is well established (Born and Bradley, 2005; Zeki, 2015), but the manner in which individual differences in MT responsiveness relate to differences in perception is less clear. In a seminal study, Rees et al. (2000) demonstrated a positive linear relationship between the coherence of moving dot stimuli and the fMRI response in human MT. They also reported modest individual variability in the coherence-response function, but not whether such variability corresponds to differences in perception. A more recent study has found a correspondence between improved behavioral performance and fMRI response changes in MT following perceptual learning (Chen et al., 2017). Specifically, subjects with smaller thresholds in a motion discrimination paradigm following extensive training also showed greater sharpening of tuning within MT, as assessed by multi-voxel pattern analysis. This suggests that increased selectivity within MT is important for learning to perform a motion discrimination task.

Here, we used a variation of a well-established motion discrimination paradigm (Foss-Feig et al., 2013; Tadin, 2015; Tadin et al., 2003), in which larger neural responses (particularly within area MT) are thought to facilitate motion direction discrimination for more-briefly presented stimuli, resulting in shorter duration thresholds (i.e., better performance). Evidence for the role of neural activity in MT within this paradigm has been provided by studies in both macaques (Liu et al., 2016) and humans (Schallmo et al., 2018; Tadin et al., 2011; Turkozer et al., 2016). Our current findings build upon this work and suggest that individual differences in Glu concentration in area MT contribute to the neural responsiveness within the region, as well as consequent motion discrimination performance. Further, we find that the 3-way association between higher Glx, stronger fMRI responses, and better motion discrimination appears specific to area MT; such relationships were not observed for Glx and fMRI measures in EVC, nor for Glx in FPC. This finding may reflect the privileged role played by neurons in MT during motion perception. Our work demonstrates how measuring Glu may provide valuable insight into the neural basis of individual differences in

visual perception.

Acknowledgments

We thank Anastasia V. Flevaris for help with data acquisition and analysis. We also thank Brenna Boyd, Judy Han, Heena Panjwani, Micah Pepper, Meaghan Thompson, Anne Wolken, and the UW Diagnostic Imaging Center for help with subject recruitment and/or data collection. Finally, we thank the anonymous reviewers for their helpful comments.

This work was supported by funding from the National Institutes of Health (F32 EY025121 to MPS, R01 MH106520 to SOM, T32 EY00703). This work applies tools developed under NIH grants R01 EB016089 and P41 EB015909; RAEE also receives support from these grants.

The authors declare that they have no competing interests with regard to the publication of this manuscript.

Appendix A. Supplementary data

Supplementary data to this article can be found online at https://doi.org/10.1016/j.neuroimage.2018.10.001.

References

Albrecht, J., Sidoryk-Wegrzynowicz, M., Zielinska, M., Aschner, M., 2011. Roles of glutamine in neurotransmission. Neuron Glia Biol. 6, 263–276.
Apšvalka, D., Gadie, A., Clemence, M., Mullins, P.G., 2015. Event-related dynamics of glutamate and BOLD effects measured using functional magnetic resonance spectroscopy (fMRS) at 3 T in a repetition suppression paradigm. Neuroimage 118, 292–300.
Born, R.T., Bradley, D.C., 2005. Structure and function of visual area MT. Annu. Rev. Neurosci. 28, 157–189.
Boynton, G.M., Demb, J.B., Glover, G.H., Heeger, D.J., 1999. Neuronal basis of contrast discrimination. Vis. Res. 39, 257–269.
Brainard, D., 1997. The psychophysics toolbox. Spatial Vis. 10, 433–436.
Britten, K.H., Shadlen, M.N., Newsome, W.T., Movshon, J.A., 1992. The analysis of visual motion: a comparison of neuronal and psychophysical performance. J. Neurosci. 12, 4745–4765.
Chen, N., Lu, J., Shao, H., Weng, X., Fang, F., 2017. Neural mechanisms of motion perceptual learning in noise. Hum. Brain Mapp. 38, 6029–6042.
Churan, J., Khawaja, F.A., Tsui, J.M., Pack, C.C., 2008. Brief motion stimuli preferentially activate surround-suppressed neurons in macaque visual area MT. Curr. Biol. 18, R1051–R1052.
Conti, F., Weinberg, R.J., 1999. Shaping excitation at glutamatergic synapses. Trends Neurosci. 22, 451–458.
Cooper, A.J.L., Kristal, B.S., 1997. Multiple roles of glutathione in the central nervous system. Biol. Chem. 378, 793–801.
Duncan, N.W., Wiebking, C., Northoff, G., 2014. Associations of regional GABA and glutamate with intrinsic and extrinsic neural activity in humans—a review of multimodal imaging studies. Neurosci. Biobehav. Rev. 47, 36–52.
Edden, R.A.E., Puts, N.A.J., Harris, A.D., Barker, P.B., Evans, C.J., 2014. Gannet: a batch-processing tool for the quantitative analysis of gamma-aminobutyric acid-edited MR spectroscopy spectra: Gannet: GABA Analysis Toolkit. J. Magn. Reson. Imag. 40, 1445–1452.
Evans, C.J., McGonigle, D.J., Edden, R.A.E., 2010. Diurnal stability of γ-aminobutyric acid concentration in visual and sensorimotor cortex. J. Magn. Reson. Imag. 31, 204–209.
Foss-Feig, J.H., Tadin, D., Schauder, K.B., Cascio, C.J., 2013. A substantial and unexpected enhancement of motion perception in autism. J. Neurosci. 33, 8243–8249.
Greenhouse, I., Noah, S., Maddock, R.J., Ivry, R.B., 2016. Individual differences in GABA content are reliable but are not uniform across the human cortex. Neuroimage 139, 1–7.
Harris, A.D., Puts, N.A.J., Edden, R.A.E., 2015. Tissue correction for GABA-edited MRS: considerations of voxel composition, tissue segmentation, and tissue relaxations: tissue Correction for GABA-Edited MRS. J. Magn. Reson. Imag. 42, 1431–1440.
Harris, A.D., Saleh, M.G., Edden, R.A.E., 2017. Edited 1H magnetic resonance spectroscopy in vivo: methods and metabolites. Magn. Reson. Med. 77, 1377–1389.
Huk, A.C., Dougherty, R.F., Heeger, D.J., 2002. Retinotopy and functional subdivision of human areas MT and MST. J. Neurosci. 22, 7195–7205.
Huk, A.C., Ress, D., Heeger, D.J., 2001. Neuronal basis of the motion aftereffect reconsidered. Neuron 32, 161–172.
Huk, A.C., Shadlen, M.N., 2005. Neural activity in macaque parietal cortex reflects temporal integration of visual motion signals during perceptual decision making. J. Neurosci. 25, 10420–10436.
Kingdom, F.A.A., Prins, N., 2010. Psychophysics: a Practical Introduction. Academic Press, London.
Kleiner, M., Brainard, D., Pelli, D., 2007. What's new in Psychtoolbox-3? Perception 36, 1.
Lin, Y., Stephenson, M.C., Xin, L., Napolitano, A., Morris, P.G., 2012. Investigating the metabolic changes due to visual stimulation using functional proton magnetic resonance spectroscopy at 7 T. J. Cerebr. Blood Flow Metabol. 32, 1484–1495.
Liu, L.D., Haefner, R.M., Pack, C.C., 2016. A neural basis for the spatial suppression of visual motion perception. eLife 5, e16167.
Logothetis, N.K., 2008. What we can do and what we cannot do with fMRI. Nature 453, 869.
Logothetis, N.K., Pauls, J., Augath, M., Trinath, T., Oeltermann, A., 2001. Neurophysiological investigation of the basis of the fMRI signal. Nature 412, 150–157.
Magistretti, P.J., Pellerin, L., Rothman, D.L., Shulman, R.G., 1999. Energy on demand. Science 283, 496–497.
Mangia, S., Tkáč, I., Gruetter, R., Van de Moortele, P.-F., Maraviglia, B., Uğurbil, K., 2007. Sustained neuronal activation raises oxidative metabolism to a new steady-state level: evidence from 1H NMR spectroscopy in the human visual cortex. J. Cerebr. Blood Flow Metabol. 27, 1055–1063.
Mescher, M., Merkle, H., Kirsch, J., Garwood, M., Gruetter, R., 1998. Simultaneous in vivo spectral editing and water suppression. NMR Biomed. 11, 266–272.
Mullins, P.G., McGonigle, D.J., O'Gorman, R.L., Puts, N.A.J., Vidyasagar, R., Evans, C.J., Edden, R.A.E., 2014. Current practice in the use of MEGA-PRESS spectroscopy for the detection of GABA. Neuroimage 86, 43–52.
Murray, S.O., Schallmo, M.-P., Kolodny, T., Millin, R., Kale, A.M., Thomas, P., Rammsayer, T.H., Troche, S.J., Bernier, R.A., Tadin, D., 2018. Sex differences in visual motion processing. Curr. Biol. 28, 2794–2799.
Near, J., Ho, Y.-C.L., Sandberg, K., Kumaragamage, C., Bilcher, J.U., 2014. Long-term reproducibility of GABA magnetic resonance spectroscopy. Neuroimage 99, 191–196.
Newsome, W.T., Britten, K.H., Movshon, J.A., 1989. Neuronal correlates of a perceptual decision. Nature 341, 52–54.
Pelli, D., 1997. The VideoToolbox software for visual psychophysics: transforming numbers into movies. Spatial Vis. 10, 437–442.
Prins, N., Kingdom, F.A.A., 2009. Palamedes: Matlab Routines for Analyzing Psychophysical Data.
Pugh, K.R., Frost, S.J., Rothman, D.L., Hoeft, F., Del Tufo, S.N., Mason, G.F., Molfese, P.J., Mencl, W.E., Grigorenko, E.L., Landi, N., 2014. Glutamate and choline levels predict individual differences in reading ability in emergent readers. J. Neurosci. 34, 4082–4089.
Rees, G., Friston, K., Koch, C., 2000. A direct quantitative relationship between the functional properties of human and macaque V5. Nat. Neurosci. 3, 716.
Schaller, B., Mekle, R., Xin, L., Kunz, N., Gruetter, R., 2013. Net increase of lactate and glutamate concentration in activated human visual cortex detected with magnetic resonance spectroscopy at 7 tesla. J. Neurosci. Res. 91, 1076–1083.
Schallmo, M.-P., Kale, A.M., Millin, R., Flevaris, A.V., Brkanac, Z., Edden, R.A.E., Bernier, R.A., Murray, S.O., 2018. Suppression and facilitation of human neural responses. eLife 7, e30334.
Tadin, D., 2015. Suppressive mechanisms in visual motion processing: from perception to intelligence. Vis. Res. 115, 58–70.
Tadin, D., Lappin, J.S., Gilroy, L.A., Blake, R., 2003. Perceptual consequences of centre–surround antagonism in visual motion processing. Nature 424, 312–315.
Tadin, D., Silvanto, J., Pascual-Leone, A., Battelli, L., 2011. Improved motion perception and impaired spatial suppression following disruption of cortical area MT/V5. J. Neurosci. 31, 1279–1283.
Takeuchi, T., Yoshimoto, S., Shimada, Y., Kochiyama, T., Kondo, H.M., 2017. Individual differences in visual motion perception and neurotransmitter concentrations in the human brain. Phil. Trans. R. Soc. B 372, 20160111.
Terhune, D.B., Murray, E., Near, J., Stagg, C.J., Cowey, A., Cohen Kadosh, R., 2015. Phosphene perception relates to visual cortex glutamate levels and covaries with atypical visuospatial awareness. Cerebr. Cortex 25, 4341–4350.
Tootell, R.B., Reppas, J.B., Dale, A.M., Look, R.B., Sereno, M.I., Malach, R., Brady, T.J., Rosen, B.R., 1995. Visual motion aftereffect in human cortical area MT revealed by functional magnetic resonance imaging. Nature 375, 139–141.
Turkozer, H.B., Pamir, Z., Boyaci, H., 2016. Contrast affects fMRI activity in middle temporal cortex related to center–surround interaction in motion perception. Front. Psychol. 7.
Wijtenburg, S.A., West, J., Korenic, S.A., Kuhney, F., Gaston, F.E., Chen, H., Roberts, M., Kochunov, P., Hong, L.E., Rowland, L.M., 2017. Glutamatergic metabolites are associated with visual plasticity in humans. Neurosci. Lett. 644, 30–36.
Yousry, T.A., Schmid, U.D., Alkadhi, H., Schmidt, D., Peraud, A., Buettner, A., Winkler, P., 1997. Localization of the motor hand area to a knob on the precentral gyrus. Brain 120, 141–157.
Zeki, S., 2015. Area V5—a microcosm of the visual brain. Front. Integr. Neurosci. 9, 21.